UV Resonance Raman Evidence for Vibrationally Independent Protoporphyrin IX Vinyl Groups

Valentino L. DeVito,[†,⊥] Ming-Zhi Cai,[‡] Sanford A. Asher,*[,†] Lisa A. Kehres,[§] and Kevin M. Smith[§]

Department of Chemistry, University of Pittsburgh, Pittsburgh, Pennsylvania 15260; Department of Chemistry, University of California, Los Angeles, California 90024; Department of Chemistry, University of California, Davis, California 95616; and Calgon Corporation, Pittsburgh, Pennsylvania 15230
(Received: November 18, 1991; In Final Form: February 18, 1992)

We have examined the protoporphyrin IX (PP) peripheral vinyl C=C stretching 220-nm-excited resonance Raman cross sections, depolarization ratios, and vinyl stretching frequencies. The depolarization ratio of 0.33 observed for the bis(cyanide) complexes of both PP and a monovinylporphyrin derivative indicates that the enhancement of the vinyl vibration is likely in both cases to be dominated by a single tensor component in a manner similar to that for the C=C stretch of simpler olefins. The data suggest that the two peripheral vinyl groups are vibrationally uncoupled.

Introduction

The peripheral vinyl groups of the protoporphyrin IX (PP) ring have been suggested to mediate heme–protein interactions in a variety of heme proteins.[1-5] In principle, these vinyl substituents could interact electronically with the aromatic heme ring and influence heme ligand binding affinities and oxidation–reduction potentials.[2,6] A number of techniques including theoretical calculations,[1-3] chemical modification studies,[6-9] NMR spectroscopy,[10-13] and resonance Raman spectroscopy[14-22] have been utilized to elucidate the role of the vinyls in modulating heme reactivity.

A direct correlation between ligand affinities and substituent electronegativity was found[6] by chemically modifying the substituent pattern around the porphyrin ring, i.e., by a systematic replacement of the vinyl groups with a host of other groups of differing electronegativities such as formyl, acetyl, and methyl. Thus, peripheral substituents can influence heme reactivity. Several laboratories, considering that the vinyl moieties in various heme proteins could assume a wide range of dihedral angles relative to the heme ring, proposed a steric model of vinyl group influences.[5,23,24] They suggested that the protein steers the vinyl orientations relative to the heme ring due to specific interactions with the amino acid residues lining the heme binding pocket. If the vinyl group were forced to become coplanar, more effective π orbital overlap would occur between the heme and vinyl π orbitals, and the electron-withdrawing nature of the vinyls would make the iron center less basic and thus more reactive to nucleophilic ligands.

Recent calculations of the π orbital interactions between the vinyl groups and the heme ring of PP by Findsen et al.[3] contradict these assumptions and conclude that little or no ground-state π orbital conjugation exists between the vinyl and the heme regardless of vinyl orientation. Furthermore, our previous UV resonance Raman excitation profile study of PP complexes, which showed selective enhancement of the 1622-cm^{-1} vinyl C=C stretch with excitation between 220 and 300 nm, proved the existence of the vinyl group ca. 200-nm $\pi \rightarrow \pi^*$ electronic transition.[14] This indicates that little vinyl group conjugation occurs in either the ground or the π^* porphyrin excited states.

Vibrational interactions between the two vinyls in PP have been proposed for Ni(PP) by Choi et al., who reported strong couplings between the two vinyl C=C stretches.[17] They assigned the 1634-cm^{-1} band in the Raman spectrum to an in-phase combination of vibrations and the 1620-cm^{-1} band in the IR spectrum to an out-of-phase combination. Indeed, normal-coordinate calculations for PP predict a ca. 10-cm^{-1} splitting for such interactions.[25] In contrast, resonance Raman spectra with Soret band excitation of reconstituted heme proteins indicate that the 2- and 4-vinyl substituents independently Raman scatter.[15,16] In addition, single-crystal depolarization ratio studies of metmyoglobin by Sage and co-workers concluded that no coupling occurs between the vinyl groups.[26]

Our study here uses UV resonance Raman spectroscopy to examine the electronic and vibrational interactions between the vinyl substituents and the heme ring. We examine whether coupling between the two vinyls through the heme is strong enough to correlate their electronic and nuclear motions. This latter question is important for the correct interpretation of the Raman spectra of heme proteins. UV resonance Raman (UVRR) spectroscopy is a particularly powerful technique to probe excited-state structure and dynamics.[27] In particular, the Raman depolarization ratios are sensitive to small changes in the symmetry properties of a molecule, and the depolarization ratios can be used to elucidate the Raman enhancement mechanisms.[28,29] These depolarization ratios have recently been utilized to monitor excited-state dephasing times.[30] We measure the 220-nm-excited depolarization ratios for the 1622-cm^{-1} vinyl C=C stretch in ferric complexes of protoporphyrin IX, the heme of most biological relevance, and a monovinylporphyrin, 2-methyl-2-devinylprotoporphyrin (MVPP), where the 2-vinyl substituent is replaced by an aliphatic methyl group as illustrated in Figure 1. We compare the depolarization ratios of the porphyrins to that of simple olefins. We find no evidence for correlation of motion between the vinyl groups in PP, and we reaffirm our earlier conclusion that the vinyl vibrational modes are enhanced by localized vinyl group $\pi \rightarrow \pi^*$ electronic transitions which remain effectively independent of the porphyrin π,π^* network.[14]

Experimental Section

Iron(III) protoporphyrin IX chloride (hemin), sodium cyanide, sodium perchlorate, and the olefin compounds were obtained from Aldrich Chemical Co. and used without further purification. Spectroscopic grade cyclohexane from Burdick and Jackson was used as received. Iron(III) 2-methyl-2-devinylprotoporphyrin chloride was prepared according to published methods.[31-33] The porphyrin solutions were made by first dissolving the solid with a few drops of 1 N sodium hydroxide to form the green μ-oxo dimer. After addition of deionized water, the solution was adjusted to pH 9 by addition of acid or base as required. These studies utilized a heme concentration of 0.25 mM. Sodium cyanide was added to a concentration of 0.10 M in order to form the bis(cyanide) porphyrin complex, and the internal standard sodium perchlorate was added to a concentration of 0.25 M.

Raman spectra were obtained with a pulsed Nd:YAG laser based system operating at 20 Hz with a 6-ns pulse width which provided tunable laser excitation from 217 to 800 nm. A pulsed

* To whom correspondence should be addressed.
† University of Pittsburgh.
‡ University of California, Los Angeles.
§ University of California, Davis.
⊥ Calgon Corporation.

0022-3654/92/2096-6917$03.00/0

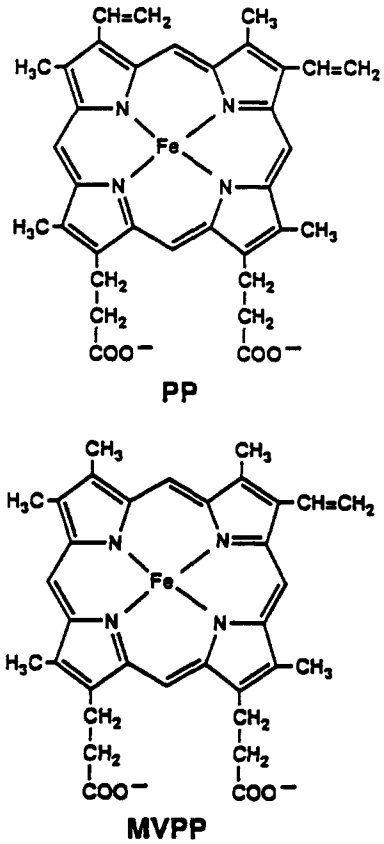

Figure 1. Molecular structure of iron(III) protoporphyin IX (PP) and iron(III) 2-methyl-2-devinylprotoporphyrin (MVPP).

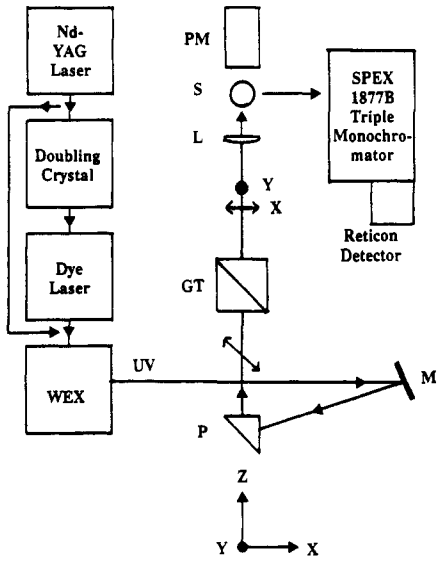

Figure 2. Schematic diagram of the Raman system used to measure UV depolarization ratios. The 1064-nm Nd:YAG fundamental is frequency doubled to pump a dye laser. This output is further frequency doubled and mixed with the IR fundamental in the WEX unit to produce UV radiation between 217 and 260 nm. A flat mirror (M) and turning prism (P) direct the beam toward the Glan-Taylor polarizing prism (GT) with a polarization in the X–Y plane but rotated 45° about the Z axis as shown. Rotation of the GT by 90° selects between the two possible incident polarizations along the X and Y axes. The lens (L) focuses the beam on the sample capillary (S). S can be reproducibly translated in and out of the beam in order to measure the incident power for each polarization orientation with the power meter (PM). The scattered light is collected at 90°. The monochromator and detector are described in the text.

excimer laser system operating at 200 Hz with a 16-ns pulse width provided the 210-nm excitation used for the depolarization ratio measurement of 1-hexene. The Raman spectrometer is described in detail elsewhere.[34,35] Aqueous samples were recirculated by a peristaltic pump through a 1.0-mm-i.d. Suprasil quartz capillary. For nonaqueous solutions a magnetic gear pump with Teflon tubing was utilized. The samples were replaced after measurements of the two 10-min Raman spectra required for a depolarization ratio measurement. UV–vis absorption spectra were measured with a Perkin-Elmer Lambda 9 spectrophotometer; no absorption spectral changes occurred due to laser excitation.

Due to the low UV transmittance of conventional dichroic sheet polarization analyzers, we measured the depolarization ratios by rotating the incident beam polarization as shown in Figure 2. An ellipsoidal mirror directed the scattered light into a 0.64-m Spex Triplemate monochromator with a Model 1420 PAR multichannel array detector. A Model 361 Scientech power meter head was positioned directly above the sample. The sample capillary was reproducibly translated in and out of the beam in order to measure the actual power delivered to the sample. The incident beam power was monitored before and after each scan, and spectral measurements that were accompanied by beam power drifts of more than 10% were discarded. The depolarization ratio, ρ, is calculated from[36-38]

$$\rho = I_X/(2I_Y - I_X) \qquad (1)$$

where I_X and I_Y are the total scattered intensities collected with the incident beam electric field polarization in the X and Y laboratory frame directions (Figure 2).

The greatest source of systematic error in our depolarization ratio determinations derives from misalignment of the incident beam polarization due to the beam convergence which results from focusing of the incident beam on the sample (Figure 2). This relatively modest polarization misalignment is a serious source of error in absorbing samples due to the decreased scattering volume due to self-absorption which increasingly weights incident rays at larger incident converging angles. Smaller systematic errors in depolarization ratio measurements result from the finite solid angle of collection of the Raman scattered radiation. We correct the observed depolarization ratios by using depolarization ratio internal standards (vide infra).

We observe negligible depolarization ratio errors for nonabsorbing solutions. For 220-nm excitation we measure depolarization ratios of 0.04 for the perchlorate 932-cm^{-1} symmetric ν_1 stretch and 0.07 for the CN^- 2076-cm^{-1} symmetric C≡N stretch (Table II). For the symmetric ν_2 bending vibration of water at ca. 1640 cm^{-1} we measure a depolarization ratio of 0.40. Previous measurements with visible wavelength excitation of the depolarization ratio for this relatively weak water band varied from ca. 0.4 to 0.6.[39-41] We measure a depolarization ratio of 0.76 for the 2150-cm^{-1} band of liquid water while Walrafen and Blatz report a value of 0.8 for this band with visible excitation.[40] This band has been assigned as $\nu_2 + \nu_L$, where ν_L refers to the librational modes of liquid water which occur between 300 and 600 cm^{-1}.[40,41]

The olefin compounds were measured as dilute solutions in cyclohexane. For cyclohexane at 220-nm excitation we obtain depolarization ratios of 0.11 and 0.74 for the polarized 802-cm^{-1} ν_5 mode and the depolarized 1445-cm^{-1} ν_{11} mode. For the set of CH stretches between 2600 and 3100 cm^{-1}, we obtain a depolarization ratio of 0.24 with 220-nm excitation (Table II). The C–H stretch depolarization ratio is in excellent agreement with the measurements of Li and Myers, who report a 218-nm depolarization ratio of 0.23.[42,43] Further, Lorenzo et al. report values of 0.107 and 0.728 for the 802- and 1445-cm^{-1} modes of cyclohexane with visible wavelength excitation.[44] Cyclohexane is a useful depolarization ratio standard for UV and visible Raman studies since no dispersion apparently occurs in its depolarization ratios between 200- and 514.5-nm excitations.

For nonabsorbing samples only small errors occur in our depolarization ratio measurements. In contrast, absorbing samples show much larger depolarization ratio errors. We therefore correct our spectral data with the measured depolarization ratios of the internal standard bands. The depolarization ratio error derives from the errors due to imperfect incident beam polarization orientation along the X and Y axes. Thus

$$I_X^{obs} = 2\frac{I_\perp}{I_\perp + I_\parallel} I_X^0 + \frac{I_\parallel}{I_\perp + I_\parallel}\Delta I_Y$$

$$I_Y^{obs} = \frac{I_\parallel}{I_\perp + I_\parallel} I_Y^0 + \frac{I_\perp}{I_\perp + I_\parallel} I_Y^0 + 2\frac{I_\perp}{I_\perp + I_\parallel}\Delta I_X \quad (2)$$

where the observed I_X^{obs} and I_Y^{obs} intensities depend on the incident beam intensities along X and Y, I_X^0 and I_Y^0, and where $I_\perp$ and $I_\parallel$ are defined by the relative ratio of Raman intensities defined by the 90° scattering depolarization ratio $\rho = I_\perp/I_\parallel$. Assuming $I_X^0 = I_Y^0$, and defining q_x and q_y as the relative errors due to misalignment of the incident beam polarizations, $\Delta I_Y/I_X^0$ and $\Delta I_X/I_Y^0$, and solving for ρ_{obs} we find

$$\rho_{obs} = \frac{2\rho + q_x}{2 + 4\rho q_y - q_x} \quad (3)$$

Clearly in the limit that q_x and q_y approach zero, ρ_{obs} becomes the true depolarization ratio ρ. For small depolarization ratios ρ_{obs} is dominated by the error due to q_x. For small ρ we simplify eq 3 to

$$\rho_{obs} = \rho\left(\frac{2}{2 - q_x}\right) + \frac{q_x}{2 - q_x} \quad (4)$$

Plots of ρ_{obs} versus ρ for these four internal standard depolarization ratios were least-squares fit to a straight line for each set of spectra. The average values of the slope and intercept in typical measurements are 1.10 and 0.072. We correct the observed porphyrin depolarization ratios for systematic errors by least-squares fitting our internal standard depolarization ratios to eq 4 and interpolating the true porphyrin depolarization ratios from these fits. The stochastic error limits are standard deviations calculated from replicate spectral measurements ($\pm 2\sigma$). This uncertainty results from the signal-to-noise ratios of the spectra.

Total differential Raman cross sections are calculated by the method of Dudik et al.[45] Since our experimental bandwidths are instrumentally limited, the depolarization ratios were determined from measured peak heights, except for the CH stretching region of cyclohexane where we utilized integrated peak areas between 2600 and 3100 cm^{-1}. Band frequencies were calibrated with acetonitrile and are accurate to ± 5 cm^{-1}.

Results and Discussion

Figure 3 shows the absorption spectra of bis(cyanide) complexes of ferric derivatives of protoporphyrin IX and 2-methyl-2-devinylprotoporphyrin (MVPP) in aqueous solution at pH 9. For the low-spin, bis(cyanide) aqueous complex of protoporphyrin IX, $(CN)_2Fe^{III}(PP)^-$, a single Q band is found at 546 nm. The Soret band (B) maximum occurs at 422 nm along with higher lying porphyrin $\pi \rightarrow \pi^*$ transitions at 363 (N) and 262 nm (L). A band also occurs at ca. 212 nm. The decrease to a single vinyl group in MVPP results in a ca. 4-nm blue shift in the λ_{max} values compared to PP, while octaethylporphyrin (OEP) shows an 8-nm blue shift (not shown). The bis(cyanide) complex of monovinylporphyrin, $(CN)_2Fe^{III}(MVPP)^-$, shows bands at 542 (Q), 418 (B), 357 (N), and ca. 260 nm (L). However, the molar absorptivity of the MVPP complex in the region from 210 to 300 nm is decreased from that of PP. The 220-nm molar absorptivities of these adducts are 4.2×10^4 and 4.7×10^4 M^{-1} cm^{-1}, respectively, while the Soret bands show molar absorptivities of 8.8×10^4 and 9.0×10^4 M^{-1} cm^{-1}, respectively. Table I, which lists the absorption spectral parameters for PP, MVPP, and OEP complexes, indicates that the molar absorptivity ratio between the Soret band maximum and that at 220 nm decreases as the number of vinyl groups on the ring increases. We previously demonstrated that little mixing occurs between the vinyl π and π^* orbitals and the heme orbitals;[14] the ca. 400-nm PP Soret transition remains overwhelmingly Soret in character, and the ca. 220-nm vinyl $\pi \rightarrow \pi^*$ transition remains predominately vinyl in character.

With 220-nm excitation the total differential Raman cross section for the vinyl mode of the bis(cyanide) ferric complexes of protoporphyrin IX is 0.16 b/str per porphyrin ring but decreases by almost 2-fold in 2-methyl-2-devinylprotoporphyrin to 0.077 b/str per porphyrin ring. These results suggest that the vinyl groups independently Raman scatter. Figure 4 shows the 220-nm-excited Raman spectra of $FePP(CN)_2^-$ and $FeMVPP(CN)_2^-$ with orthogonal incident beam polarizations. The contributions from the internal standard bands and the 1640-cm^{-1} symmetric bend (ν_2) of water have been numerically removed. The UV

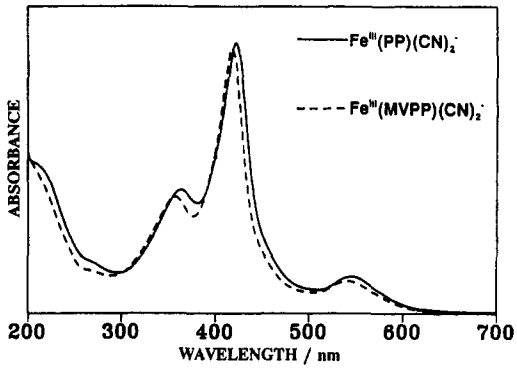

Figure 3. Absorption spectra of the bis(cyanide) complexes of PP (—) and MVPP (---) at pH 9. Sample concentrations are 0.25 mM. The path length of the cell is 0.05 cm.

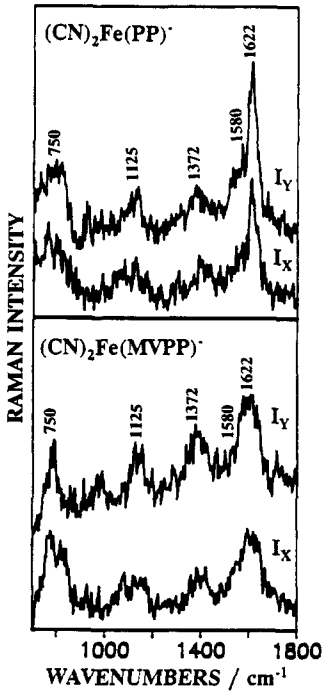

Figure 4. The 220-nm-excited UV resonance Raman depolarization ratio measurements of $(CN)_2Fe(PP)^-$ and $(CN)_2Fe(MVPP)^-$. The pulse energy flux at the sample is ~1.5 mJ/cm^2. The water and internal standard band contributions have been numerically subtracted out. The broader bands for the MVPP complex result from an increased monochromator slit width. Note that these are the spectra obtained using the different incident polarizations. The actual depolarization ratios are calculated from fits which utilize the depolarization ratio internal standards as discussed in the text.

TABLE I: Absorption Spectral Data for Comparison of Protoporphyrin IX, Monovinylporphyrin, and Octaethylporphyrin Complexes

porphyrin	Soret max λ/nm	$\epsilon_{Soret}/\epsilon_{220}$[a]
Fe(PP)Cl[b]	398	5.5
Fe(MVPP)Cl[b]	393	6.3
Fe(OEP)Cl[b]	390	7.3

[a] Molar absorptivity ratios measured from peak heights. [b] Measured as dilute solutions in methanol.

TABLE II: UV Raman Depolarization Ratios[a]

molecule	freq (cm^{-1})	excitation (nm) 210	220	251
$(CN)_2Fe(PP)^-$	1622		0.37 ± 0.05[b]	
	1372		0.2 ± 0.1	
	1125		0.4 ± 0.1	
$(CN)_2Fe(MVPP)^-$	1622		0.37 ± 0.06	
	1372		0.3 ± 0.1	
	1125		0.3 ± 0.1	
cyclohexane	802	0.15 ± 0.02	0.11 ± 0.01	0.10 ± 0.02
	1029	0.76 ± 0.07	0.80 ± 0.16	0.71 ± 0.07
	1268	0.74 ± 0.07	0.77 ± 0.03	0.74 ± 0.07
	1445	0.76 ± 0.06	0.74 ± 0.05	0.74 ± 0.09
	2600–3100	0.24 ± 0.02		
1-hexene	1641	0.26 ± 0.02	0.20 ± 0.03	0.14 ± 0.03
1,3-hexadiene	1651		0.41 ± 0.06	0.33 ± 0.03
1,3,5-hexatriene	1635		0.36 ± 0.02	0.37 ± 0.03
vinylcyclohexane	1642		0.22 ± 0.03	
tetrachloro-ethylene	1574		0.36 ± 0.05	
acetonitrile	918		0.08 ± 0.02	
	1376		0.45 ± 0.06	
	2249		0.12 ± 0.02	
water	1640		0.40 ± 0.06	
	2150		0.76 ± 0.07	
perchlorate	932		0.04 ± 0.02	
cyanide	2076		0.07 ± 0.03	
sulfate	981		0.03 ± 0.01	
selenate	834		0.04 ± 0.02	
nitrate	1045		0.19 ± 0.05	
cacodylic acid	605		0.20 ± 0.04	

[a] All 220- and 251-nm depolarization ratios were measured using the Glan-Taylor prism as described in Figure 2. The 210-nm data were measured with the use of a calibrated Polacoat analyzer (see ref 14). [b] The present value is somewhat less than that which we measured previously using the lower signal-to-noise Polacoat analyzer technique.[14]

Raman bands observed include the 1622-cm^{-1} vinyl C=C stretch, the ca. 1580-cm^{-1} ν_2 mode, the 1372-cm^{-1}, ν_4 mode, and the 750-cm^{-1} ν_{16} in-plane pyrrole C_aNC_a deformation.[14,17,18] The 1125-cm^{-1} mode involves vinyl–heme stretching as well as motion of the vinyl relative to the heme ring and vinyl CH_2 and heme ring motions.[14,25] The frequency and bandwidth of the 1622-cm^{-1} vinyl stretch are essentially identical between PP and MVPP bis(cyanide) complexes as evident from spectra obtained at higher resolution than those shown in Figure 4.

The measured depolarization ratios of the porphyrin complexes and other species are listed in Table II. For the 1622-cm^{-1} vinyl C=C stretch of $(CN)_2Fe^{III}(PP)^-$ and $(CN)_2Fe^{III}(MVPP)^-$ we obtain depolarization values of 0.37 ± 0.05 and 0.37 ± 0.06, in agreement with the value of 0.33 expected for resonance enhancement within a single isolated C=C $\pi \rightarrow \pi^*$ electronic transition. We earlier presented data which indicated that selective UV enhancement of vinyl modes in PP occurs because the vinyl $\pi \rightarrow \pi^*$ electronic transitions are electronically isolated and not conjugated with the heme ring.

We expect a resonance Raman depolarization ratio of 0.33 for a C=C stretch if it is resonance enhanced by a single nondegenerate linearly polarized electronic transition. We expect a resonance Raman depolarization ratio of 0.33 for the vinyl stretch of 1-hexene with excitation into its ca. 180-nm $\pi \rightarrow \pi^*$ transition. In contrast, with 220-nm preresonance Raman excitation we measure depolarization ratios of 0.20 ± 0.03 and 0.22 ± 0.03 for 1-hexene and vinylcyclohexane, respectively. We presume that the lowered depolarization ratios for these compounds result from the lack of exact resonance with the $\pi \rightarrow \pi^*$ transition and the resulting significant contribution of higher electronic transitions to the preresonance enhancement. This is supported by the dispersion of the depolarization ratio for these compounds. The depolarization ratio for 1-hexene varies from 0.07 at 415 nm to 0.14 at 251 nm, 0.20 at 220 nm, and 0.26 at 210 nm. This dispersion is likely to result in a depolarization ratio of 0.33 upon excitation within the ca. 180-nm $\pi \rightarrow \pi^*$ vinyl transition. Further, as Table II indicates, resonance excitation within the $\pi \rightarrow \pi^*$ transition of 1,3-hexadiene, 1,3,5-hexatriene, and tetrachloroethylene results in ca. 0.33 depolarization ratio values.[46,47] Furthermore, resonance excitation into the $\pi \rightarrow \pi^*$ transitions of β-carotene and *trans*-retinal results in ~0.33 depolarization ratio values.[48,49]

TABLE III: Angles between Vinyl Axes and Calculated Depolarization Ratios for Protoporphyrin IX

complex	θ^a	$\rho_{in\text{-}phase}$	$\rho_{out\text{-}of\text{-}phase}$	ref
$(1\text{-MeIm})_2Fe(PP)^+$	25	0.31	0.75	50
$(p\text{-}SC_6H_4NO_2)Fe(PPDME)^{+b}$	70	0.16	0.75	51
H_2PPDME	78	0.14	0.75	52
deoxy-Mb	87	0.13	0.75	5MBN[c]
metMb	86	0.13	0.75	4MBN[c]

[a] Calculated from atomic coordinates; angle in degrees. [b] PPDME is the dimethyl ester of PP. [c] From Brookhaven Protein Data Bank.

The observed resonance Raman depolarization ratio of 0.33 conveys information on whether the vinyl groups are electronically and/or vibrationally coupled. Four possible cases can occur: (1) the vinyl groups are neither electronically nor vibrationally coupled; (2) the vinyl groups are not electronically coupled but are vibrationally coupled; (3) the vinyl groups are electronically but not vibrationally coupled; and (4) the vinyl groups are both electronically and vibrationally coupled.

For case 1 the vinyl electronic and vibrational motion is uncorrelated and the vinyls scatter independently, as if they were on separate molecules. The tensor elements add at the amplitude-squared (intensity) level. Thus, only one tensor element exists, and a depolarization ratio of 0.33 will occur. For case 2 vibrational coupling results in the formation of two vibrations, where vinyl motion occurs either in-phase or out-of-phase. The Raman intensity of these vibrations derives from enhancements of these two vibrational modes (associated with in-phase and out-of-phase vinyl stretching) each by both vinyl $\pi \rightarrow \pi^*$ electronic transitions. Each vibration is enhanced by both transitions, and for each vibration two tensor elements exist which add at the amplitude level. A frequency difference will occur between the in-phase and out-of-phase coupled vibration. Case 3, where the electronic transitions are coupled and the vinyls vibrate independently, shows a Raman tensor with only one element and a depolarization ratio of 0.33. The frequencies of the two vibrations will be identical. In case 4, the Raman tensor will have two elements in the diagonal frame. The vinyl frequencies will differ between the in-phase and out-of-phase vibrational mode.

The Raman tensor for cases 2 and 4 for the in-phase or out-of-phase coupled vinyl vibrations can be written

$$\alpha_{vinyl,1} \pm \alpha_{vinyl,2} = \alpha \begin{pmatrix} 1 \pm \cos^2\theta & \pm\cos\theta \sin\theta & 0 \\ \pm\cos\theta \sin\theta & \pm\sin^2\theta & 0 \\ 0 & 0 & 0 \end{pmatrix} \quad (5)$$

where α is the dominant scattering tensor component for a single vinyl group, θ is the angle between the two vinyl C=C axes in PP, and the positive sign is used for the in-phase coupling combination. In the diagonal frame the in-phase combination tensor is

$$\alpha \begin{pmatrix} 1 + \cos\theta & 0 & 0 \\ 0 & 1 - \cos\theta & 0 \\ 0 & 0 & 0 \end{pmatrix} \quad (6)$$

while the out-of-phase combination tensor is

$$\alpha \begin{pmatrix} \sin\theta & 0 & 0 \\ 0 & -\sin\theta & 0 \\ 0 & 0 & 0 \end{pmatrix} \quad (7)$$

The out-of-phase tensor yields a depolarization ratio of 0.75 independent of angle.

The calculated angular dependence of the in-phase depolarization ratio is shown in Figure 5. As θ increases from 0° to 90°,

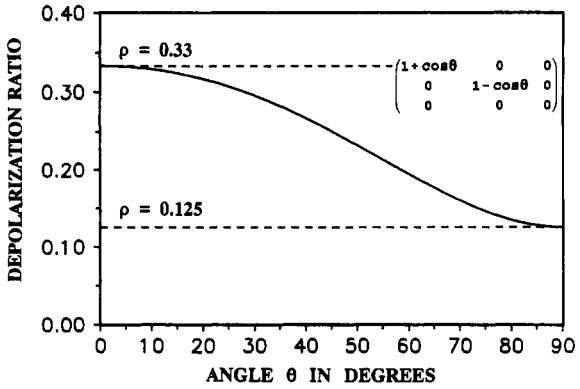

Figure 5. Plot of the dependence of the in-phase scattering tensor depolarization ratio on the angle θ between the vinyl groups. For small angles the depolarization ratio approaches 0.33, while at 90° the depolarization ratio becomes 0.125.

ρ decreases from 0.33 to 0.125. Table III lists the calculated angles between the vinyl groups found for PP derivatives from the literature and from protein X-ray crystal structures found in the Brookhaven Protein Data Bank. Our measured depolarization ratio values rule out cases 2 and 4 for those derivatives with large values of θ such as iron(III) (*p*-nitrobenzenethiolate)protoporphyrin IX dimethyl ester, free base protoporphyrin IX dimethyl ester, and sperm whale deoxy-Mb and metMb; however, the precision of our depolarization ratios does not let us rule out in-phase electronic coupling and/or vibrational coupling for iron(III) bis(1-methylimidazole)protoporphyrin IX where the vinyl groups have a small 25° angle between themselves. Our results cannot rule out case 3 where electronic coupling occurs in the absence of vibrational coupling.

Our depolarization ratio results indicate that the vinyl vibrations are uncoupled. This is consistent with the additivity observed for the vinyl Raman cross sections and the fact that the vibrational frequencies of the divinyl derivatives are essentially identical to that of the monovinyl derivative. This result contrasts with the conclusions of Choi et al.,[17] who claimed to observe separate bands in the Raman and IR spectra for the in-phase and out-of-phase coupled vinyl vibrations of NiPP. They noted that the vinyl stretching frequency in the IR (solid sample) differed by 15 cm^{-1} from that in the Raman spectrum (solution sample). In contrast, Sage et al.[26] suggested independent vinyl motion from the polarization dependence of single-crystal Raman scattering of the heme of myoglobin. A lack of vibrational coupling is also evident from reconstituted insect hemoglobin studies of Gersonde et al., who observe separate Raman bands for the two vinyl stretches with Soret band excitation.[15]

The UV Raman depolarization ratios, the Raman cross sections, and the invariance of the vinyl stretching freuqencies to the existence of a second vinyl group indicate vibrationally independent vinyl groups attached to the heme ring. Our previous UV measurements indicated little or no vinyl–heme conjugation.[14] Our new results here reinforce our previous conclusion that the vinyl substituents are not likely to play a role in modulating ligand binding affinities in heme proteins. We suggest that the existence of the vinyl groups in PP derives solely from the evolutionary history of heme biosynthesis, and of course, they serve additionally as sites of heme attachment (thioether linkages) for the cytochrome *c* electron transport proteins.[53]

Conclusions

The UV resonance Raman enhancement of the vinyl stretches of protoporphyrin IX derives from resonance excitation into vinylic $\pi \rightarrow \pi^*$ electronic transitions localized on the individual vinyl peripheral groups. This enhancement is essentially identical in nature to that for vinyl groups in aliphatic olefins. The observed UV Raman depolarization ratio of 0.33 for a single vinyl group substituted heme derivative suggests that a single tensor component dominates the enhancement of the 1622-cm^{-1} vinyl stretch. Furthermore, the identical depolarization ratio 0.33 for both protoporphyrin IX with two vinyl groups and a monovinyl derivative indicates the lack of vibrational coupling between the vinyl groups of protoporphyrin IX. The alternative possibility that the angle between the vinyl groups is small appears unlikely.

Acknowledgment. We gratefully acknowledge support of this work from NIH Grants GM37041-10 (to S.A.A.) and HL22252-13 (to K.M.S.).

Registry No. $(CN)_2Fe(MVPP)^-$, 141344-42-5; $(CN)_2Fe(PP)^-$, 41127-52-0.

References and Notes

(1) Warshel, A.; Weiss, R. M. *J. Am. Chem. Soc.* **1981**, *103*, 446–451.
(2) Gelin, B. R.; Karplus, M. *Proc. Natl. Acad. Sci. U.S.A.* **1977**, *74*, 801–805.
(3) Findsen, L. A.; Bocian, D. F.; Birge, R. R. *J. Chem. Phys.* **1988**, *88*, 7588–7598.
(4) Shelnutt, J. A.; Ortiz, V. *J. Phys. Chem.* **1985**, *89*, 4733–4739.
(5) Reid, L. S.; Lim, A. R.; Mauk, A. G. *J. Am. Chem. Soc.* **1986**, *108*, 8197–8201.
(6) Asakura, T.; Lau, P. W.; Sono, M.; Adachi, K.; Smith, J. J.; McCray, J. A. *Hemoglobin and Oxygen Binding*; Ho, C., Ed.; Elsevier Biomedical: New York, 1982; pp 177–184.
(7) Gersonde, K.; Sick, H.; Overkamp, M.; Smith, K. M.; Parish, D. W. *Eur. J. Biochem.* **1986**, *157*, 393–404.
(8) Sono, M.; Asakura, T. J. *Biol. Chem.* **1975**, *250*, 5227–5232.
(9) Asakura, T.; Sono, M. J. *Biol. Chem.* **1974**, *249*, 7087–7093.
(10) Thanabal, V.; deRopp, J. S.; LaMar, G. N. *J. Am. Chem. Soc.* **1986**, *108*, 4244–4245.
(11) Bothner-By, A. A.; Gayathri, C.; van Zijl, P. C. M.; MacLean, C.; Lai, J.; Smith, K. M. *Magn. Reson. Chem.* **1985**, *23*, 935–938.
(12) LaMar, G. N.; Viscio, D. B.; Gersonde, K.; Sick, H. *Biochemistry* **1978**, *17*, 361–367.
(13) LaMar, G. N.; Burns, P. D.; Jackson, J. T.; Smith, K. M.; Langry, K. C.; Strittmatter, P. *J. Biol. Chem.* **1981**, *256*, 6075–6079.
(14) DeVito, V. L.; Asher, S. A. *J. Am. Chem. Soc.* **1989**, *111*, 9143–9152.
(15) Gersonde, K.; Yu, N. T.; Lin, S. H.; Smith, K. M.; Parish, D. W. *Biochemistry* **1989**, *28*, 3960–3966.
(16) Uchida, K.; Susai, Y.; Hirotani, E.; Kimura, T.; Yoneya, T.; Takeuchi, H.; Harada, I. J. *Biochemistry* **1988**, *103*, 979–985.
(17) Choi, S.; Spiro, T. G.; Langry, K. C.; Smith, K. M. *J. Am. Chem. Soc.* **1982**, *104*, 4337–4344.
(18) Choi, S.; Spiro, T. G.; Langry, K. C.; Smith, K. M.; Budd, D. L.; LaMar, G. N. *J. Am. Chem. Soc.* **1982**, *104*, 4345–4351.
(19) Sarkar, M.; Verma, A. L. *J. Raman Spectrosc.* **1986**, *17*, 407–414.
(20) Kerr, E. A.; Yu, N. T.; Gersonde, K.; Parish, D. W.; Smith, K. M. *J. Biol. Chem.* **1985**, *260*, 12665–12669.
(21) Rousseau, D. L.; Ondrias, M. R.; LaMar, G. N.; Kong, S. B.; Smith, K. M. *J. Biol. Chem.* **1983**, *258*, 1740–1746.
(22) Desbois, A.; Mazza, G.; Stetzkowski, F.; Lutz, M. *Biochim. Biophys. Acta* **1984**, *785*, 161–176.
(23) LaMar, G. N.; Budd, D. L.; Smith, K. M.; Langry, K. C. *J. Am. Chem. Soc.* **1980**, *102*, 1822–1827.
(24) Balke, V. L.; Walker, F. A.; West, J. T. *J. Am. Chem. Soc.* **1985**, *107*, 1226–1233.
(25) Lee, H.; Kitagawa, T.; Abe, M.; Pandy, R. K.; Leung, H. K.; Smith, K. M. *J. Mol. Struct.* **1986**, *146*, 329–347.
(26) Sage, J. T.; Morikis, D.; Champion, P. M. *J. Chem. Phys.* **1989**, *90*, 3015–3032.
(27) Asher, S. A. *Annu. Rev. Phys. Chem.* **1988**, *39*, 537–588.
(28) Mortenson, O. S.; Hassing, S. In *Advances in Infrared and Raman Spectroscopy*; Clark, R. J. H., Hester, R. E., Eds.; Wiley: Heyden, 1980; p 1.
(29) Hamaguchi, H. In *Advances In Infrared and Raman Spectroscopy*; Clark, R. J. H., Hester, R. E., Eds.; Wiley: Heyden, 1985; pp 273–310.
(30) Myers, A. B.; Hochstrasser, R. M. *J. Chem. Phys.* **1987**, *87*, 2116–2121.
(31) Smith, K. M.; Fujinari, E. M.; Langry, K. C.; Parish, D. W.; Tabba, H. D. *J. Am. Chem. Soc.* **1983**, *105*, 6638–6646.
(32) Smith, K. M.; Parish, D. W.; Inouye, W. S. *J. Org. Chem.* **1986**, *51*, 666–671.
(33) Smith, K. M.; Kehres, L. A. *J. Chem. Soc., Perkin Trans. 1* **1983**, 2329–2335.
(34) Asher, S. A.; Johnson, C. R.; Murtaugh, J. L. *Rev. Sci. Instrum.* **1983**, *54*, 1657–1662.
(35) Jones, C. M.; DeVito, V. L.; Harmon, P. A.; Asher, S. A. *Appl. Spectrosc.* **1987**, *41*, 1268–1275.
(36) Dawson, P. *Spectrochim. Acta* **1972**, *28A*, 715–723.
(37) Myers, A. B.; Li, B.; Ci, X. *J. Chem. Phys.* **1988**, *89*, 1876–1886.
(38) Li, B.; Myers, A. B. *J. Chem. Phys.* **1988**, *89*, 6658–6666.
(39) DeSantis, A.; Frattini, R.; Sampoli, M.; Mazzacurati, V.; Nardone, M.; Ricci, M. A.; Ruocco, G. *Mol. Phys.* **1987**, *61*, 1199–1212.
(40) Walrafen, G. E.; Blatz, L. A. *J. Chem. Phys.* **1973**, *59*, 2646–2650.
(41) Walrafen, G. E.; Hokmabadi, M. S.; Yang, W. H. *J. Phys. Chem.* **1988**, *92*, 2433–2438.
(42) Li, B.; Myers, A. B. *J. Phys. Chem.* **1990**, *94*, 4051–4054.
(43) Matrai, E.; Gal, M.; Keresztury, G. *Spectrochim. Acta* **1990**, *46A*, 29–32.

(44) Lorenzo, C. F.; Alcantara, R.; Martin, J. J. Raman Spectrosc. 1989, 20, 291-296.
(45) Dudik, J. M.; Johnson, C. R.; Asher, S. A. J. Chem. Phys. 1985, 82, 1732-1740.
(46) Myers, A. B.; Pranata, K. S. J. Phys. Chem. 1989, 93, 5079-5087.
(47) Udagawa, Y.; Iijima, M.; Ito, M. J. Raman Spectrosc. 1974, 2, 313-315.
(48) Inagaki, F.; Tasumi, M.; Miyazawa, T. J. Mol. Spectrosc. 1974, 50, 286-303.
(49) Doukas, A. G.; Aton, B.; Callender, R. H.; Honig, B. Chem. Phys. Lett. 1978, 56, 248-252.
(50) Little, R. G.; Dymock, K. R.; Ibers, J. A. J. Am. Chem. Soc. 1975, 97, 4532-4539.
(51) Tang, S. C.; Koch, S.; Papaefthymiou, G. C.; Foner, S.; Frankel, R. B.; Ibers, J. A.; Holm, R. H. J. Am. Chem. Soc. 1976, 98, 2414-2434.
(52) Caughey, W. S.; Ibers, J. A. J. Am. Chem. Soc. 1977, 99, 6639-6645.
(53) Stryer, L. Biochemistry, 3rd ed.; W. H. Freeman and Co.: New York, 1988; pp 404, 595.

An Investigation of Hydrogen Bonding in Amides Using Raman Spectroscopy

Nancy E. Triggs and James J. Valentini*

Department of Chemistry, Columbia University, New York, New York 10027 *(Received: December 4, 1991; In Final Form: May 11, 1992)*

Raman and preresonant Raman spectra are reported for ϵ-caprolactam and *N,N*-dimethylacetamide in both the gas phase and the neat liquid and as a function of concentration in aqueous and other solutions. These spectra are analyzed to determine the influence of hydrogen bonding, particularly amide–amide hydrogen bonding, on amide structure and spectroscopy. A shift in intensity from the Am I (carbonyl stretch) band to the Am II band (C–N stretch) is observed as the extent of intermolecular amide–amide and amide–water hydrogen bonding increases. For ϵ-caprolactam, which can hydrogen bond to itself, a substantial shift in intensity in these amide bands occurs between the gas and the neat liquid. The formation of hydrogen-bonded complexes, for which there is a clear spectral signature in the Raman spectrum, is indicated. In contrast, for *N,N*-dimethylacetamide the Am I to Am II intensity shift is seen only upon aqueous solvation and is directly proportional to the mole fraction of water present. Shifts in the Am I vibration to lower frequency are also observed upon solvation for both ϵ-caprolactam and *N,N*-dimethylacetamide whether or not hydrogen bonding is present. However, the magnitudes of these shifts increase with the extent of hydrogen bonding. The Am I carbonyl band in neat ϵ-caprolactam liquid and in acetonitrile solution consists of two peaks, one of which we assign to the unassociated monomer and the other to the cyclic dimer. In aqueous solution the carbonyl band of *N,N*-dimethylacetamide also consists of two peaks, which appear to be associated with a free and a hydrogen-bonded form.

Introduction

As the repeat unit in both biologically important macromolecules and industrially important polymeric materials, the amide functional group has long been of practical importance and fundamental interest. In an attempt to provide a better understanding of amide macromolecular systems, many studies of small, isolated amides have been reported. Indeed, a variety of techniques such as IR, NMR, Raman, ultrasonic absorption, and UV/vis spectroscopy have been used to characterize both the intermolecular and intramolecular bonding in amide compounds. From a biological standpoint, aqueous solution studies are desirable. In dilute aqueous solution, amide groups are only weakly interacting and amide–water interactions dominate.[1] However in polyamide materials, amide–amide interactions are substantial, and it is the influence of these forces on the bonding, structure, and dynamics of polyamides that interest us.

In the work described here we seek to identify Raman spectral signatures of amide–amide hydrogen bonds and exploit these to investigate hydrogen bonding in cis and trans amide conformers. Our approach is to examine the effects of phase and solvent on the Raman spectra of two prototypical amide compounds, one which can hydrogen bond to itself, ϵ-caprolactam, and one which cannot, *N,N*-dimethylacetamide. While many of our spectra are recorded upon excitation at optical frequencies far below the first electronic absorption in the amides, we do make use of preresonant enhancement of amide group vibrational modes to identify them among other modes in the spectra. Preresonant enhancement occurs in the Raman spectra that we have obtained at UV wavelengths near the very strong $\Pi \rightarrow \Pi^*$ transition characteristic of all amides.[2-4] None of the spectra we report here are recorded at Raman excitation wavelengths actually within the $\Pi \rightarrow \Pi^*$ absorption band and so are not actually resonant Raman spectra. Nonetheless, our approach is similar to the very successful use of resonance Raman spectroscopy as a conformation-sensitive probe of the nature of the ground and excited electronic states of many small peptides and proteins.[5-15]

An important consideration in our study is the type of hydrogen bond that the amides form. In N-monosubstituted amides the carbonyl oxygen and the amidic hydrogen predominantly exist in the trans conformation.[1] As a consequence, if the amidic proton in molecule A hydrogen bonds to the carbonyl of nearest-neighbor molecule B, the carbonyl of A can hydrogen bond only to a different neighbor, C, leading to the formation of long-chain oligomers of varying lengths. The presence of a variety of sizes and geometries of oligomers makes it difficult to associate specific spectral features with particular species and similarly difficult to interpret spectral signatures of hydrogen bonding. In contrast, cyclic aliphatic lactams like ϵ-caprolactam that have ring size less than eight are found only in the cis conformation, due to ring strain, and in nonpolar solvents these lactams readily form hydrogen-bonded cyclic dimers.[16-18] Thus, they offer the possibility of examining the role of amide–amide hydrogen-bonding interactions under conditions for which the hydrogen-bonded species are unique in chemical makeup and of well-defined geometry.

In this paper we report Raman spectra of ϵ-caprolactam in both the gas and liquid phase. The liquid-phase spectra are reported for neat caprolactam and solutions of caprolactam in various solvents. By monitoring both changes in band position and relative intensity with phase and solvent, we determine how interamide forces are revealed in the Raman spectrum. To separate the effects of interamide hydrogen bonding from the effects of simple solvation, we compare our caprolactam results with those for *N,N*-dimethylacetamide (DMA). Because it lacks an amidic hydrogen, DMA cannot hydrogen bond to itself, although it can and does hydrogen bond in aqueous solution. To determine how these effects vary with Raman excitation wavelength, we record Raman

0022-3654/92/2096-6922$03.00/0